

Unveiling the Structural Heterogeneity of Bamboo Lignin by In Situ HSQC NMR Technique

Jia-Long Wen · Bai-Liang Xue · Feng Xu · Run-Cang Sun

Published online: 3 June 2012
© Springer Science+Business Media, LLC 2012

Abstract One of the primary challenges for efficient utilization of lignocellulosic biomass is to clarify the complicated structure of lignin. In this study, in situ heteronuclear single quantum coherence nuclear magnetic resonance (NMR) characterization of the structural heterogeneity of lignin polymers during successively treated bamboo was emphatically performed without componential separation. Specially, the NMR spectra were successfully obtained by dissolving the acetylated and non-acetylated bamboo samples in appropriate deuterated solvent (CDCl_3 and $\text{DMSO-}d_6$). The heterogeneous lignin polymers in bamboo samples were demonstrated to be HGS-type and partially acylated at the γ -carbon of the side chain by *p*-coumarate and acetate groups. The major lignin linkages (β -O-4, β - β , and β -5, etc.) and various lignin-carbohydrate complex linkages (benzyl ether and phenyl glycoside linkages) can be assigned, and the frequencies of the major lignin linkages were quantitatively obtained. In particular, the residual enzyme lignin (REL) contained a higher amount of syringyl units and less condensed units as compared to other samples. Inspiringly, the method gives us a vision to track the structural changes of plant cell wall (e.g., lignin polymers) during the different pretreatments.

Keywords Pretreatment · Bamboo lignin · In situ NMR technique · S/G ratios · β -O-4 linkage · DMSO/NMI

Introduction

Shifting society's dependence away from petroleum to renewable biomass resources is generally viewed as an important contributor to the development of a sustainable industrial society and effective management of greenhouse gas emissions [1]. With the inevitable decrease in supply of petroleum-based resources and mitigate the pressure of greenhouse gas, lignocelluloses, such as agricultural and forest residues, have been viewed as sustainable alternative resources for producing energy and chemical feedstocks because of their huge abundance and sustainability [2]. However, one of the primary challenges for efficient utilization of lignocellulosic biomass is to clarify their complicated structure. In the past, researchers have focused on characterization of the chemical structures of various components in the plant cell walls (cellulose, hemicelluloses, and lignin). In general, waxed-free kibbling samples or ball-milling preparations are required for common isolation and spectroscopic analysis of its components. The methods have played a very significant role in plant chemistry; however, they only focus on one component of cell wall, and could not provide panoramic structural features or changes of the whole cell wall components via an un-isolated approach, i.e., in situ approach. Ideally, the chemical structure of the cell wall and its components should be identified in intact samples containing the native cell wall [2]. Thanks to the advanced nuclear magnetic resonance (NMR) techniques, the in situ characterization of plant cell wall has been primitively achieved [3]. This developed method can be used in tracing the structural changes of biomass during fungal treatments [4]. In consideration of the fact that current conversion of biomass to biofuels is detrimentally impacted by its native recalcitrance [5, 6], such as the adverse impact of lignin and hemicelluloses, the method of in situ characterization gives us

J.-L. Wen · B.-L. Xue · F. Xu (✉) · R.-C. Sun (✉)
Institute of Biomass Chemistry and Technology,
Beijing Forestry University,
Beijing 100083, China
e-mail: xfx315@163.com
e-mail: rcsun3@bjfu.edu.cn

enlightenment to track the structural changes of plant cell wall during the continuous pretreatments, especially the evolution of lignin structure during successive treatments.

Characterization of plant cell wall via NMR method was firstly proposed in 2003 by Lu and Ralph, who developed a bi-solvent system of *N*-methylimidazole (NMI) and dimethyl sulfoxide (DMSO) to dissolve finely ball-milled plant cell walls and performed detailed structural studies on the acetylated plant cell wall solutions using a high-resolution NMR spectroscopy [7]. The method opens up a new horizon to identify biomass structure, especially lignin structure. However, the complexity of spectra still hinders the unmasking of the lignin structure in situ status. Subsequently, the bi-solvent system (DMSO/NMI) was also applied to the whole lignin study [8]. The researchers remove bulk of carbohydrates to reveal the lignin structure and give us a satisfactory spectrum. However, the data obtained were only suited for softwood lignin. Afterwards, the in situ NMR technique was also applied to antiquity preservation [9, 10], in which the changes of lignin and carbohydrates in the waterlogged wood were investigated by Py-GC/MS and NMR techniques via derivatizing the wood in ionic liquid. Recently, Qu et al. [11] acetylated Fir wood in an ionic liquid and then qualitatively identified the acetylated lignin and polysaccharide signals using 2D heteronuclear single quantum coherence (HSQC) NMR technique. However, chemical modification of the plant cell wall, even simple derivatization, led to the loss of some structural information. For example, natural acetylation in the plant cell wall was masked when the sample was per-acetylated.

Along with these research avenues, structural characterization of biomass could be directly investigated by NMR investigations via non-derivatization solvent systems, such as DMSO- d_6 [12], DMSO- d_6 /NMI- d_6 [13], and DMSO- d_6 /pyridine- d_5 [3]. Based on these explorations, it was found that cell wall could not be entirely dissolved in the DMSO- d_6 but formed gel-state substance for NMR experiments. In general, the overlapped signals in the carbohydrates region seriously impacted the spectral analysis of the plant cell wall, especially in lignin polymers. Subsequently, the mixed solvents (DMSO- d_6 /NMI- d_6 and DMSO- d_6 /pyridine- d_5) were developed to improve the resolution of spectra and obtained more satisfied results. However, some overlapped and inexplicable signals still hinder the unmasking of component structural features, especially the structures of lignin polymers. Afterwards, the methodology of in situ characterization biomass was recently improved by Ragauskas' group. They firstly applied in situ characterization in evaluating the structural changes of biomass pretreatments (steam, dilute H₂SO₄, and lime at 160°C) by developing a novel bi-solvent (per-deuterated pyridinium chloride-DMSO- d_6) [5, 6]. The above-mentioned research interests enlighten us to track the structural changes of lignin polymers caused by pretreatment (regeneration) and enzymatic treatment. Most importantly, the

structural determination (acetylated and non-acetylated samples, qualitative and quantitative) of lignin polymer as well as lignin-carbohydrate complex (LCC) structure in a native state during the various treatments should be clarified via NMR techniques prior to its utilization.

Bamboo, a perennial lignified plant, belongs to the Gramineae family. According to the available data, there are 1,000 species of bamboo worldwide, and approximately 500 species can be found in China. The existing bamboo forest area in China is six million hectares according to the statistical data from the State Forestry Bureau of China. Bamboo is considered a promising biomass for pulping and bioethanol production due to its rapid growth rate and huge quantity. Recently, it was reported that the bamboo lignin could be easily released after the mild alkali treatment, and the isolated alkali lignin has been studied by wet chemistry and spectroscopic methods [14]. The well-characterized lignin fractions could be used as starting materials for developing downstream products. However, the isolated lignin could not completely represent the whole lignin of bamboo cell wall [14]. Therefore, it is necessary to reveal the heterogeneity of lignin by in situ method.

In the present study, in situ solution state 2D HSQC NMR technique was applied to investigate the structural inhomogeneity of lignin polymers (acetylated samples) in the bamboo during sequential treatments (regeneration and enzymatic hydrolysis treatment). In addition, the enzymatic hydrolysis bamboo (EB and REB, non-acetylated), which could be used as a raw material for developing lignin-based products, were subjected to in situ analysis to track the structural changes of lignin polymers and the LCC during the enzymatic treatment. Furthermore, the ball-milled bamboo undergone consecutive treatments were also analyzed by GPC to estimate the possible changes of the corresponding molecular weight distributions during the successive treatments.

Experimental

Material

Solvents (DMSO and NMI) used were AR grade and supplied by Beijing Chemical Company, Beijing, China. Deuterated chloroform was purchased from Sigma Chemical Co. (Beijing, China).

The cellulolytic enzyme used in this study was Celluclast 1.5 L, kindly supplied by Novozymes, China. It had a filter paper activity of 70 FPU/g.

Preparation of Ball-Milled Bamboo and Lignin Preparation

Bamboo, *Bambusa rigida* sp., was obtained from Sichuan, China. The bamboo culms were dried in an oven at 50°C,

followed by grinding to obtain particles with a size distribution between 450 and 900 μm (20–40 mesh). The subsequent treatment with a mixture of toluene/ethanol (2:1, v/v) in a Soxhlet extractor for 12 h removed most extractives. Klason lignin in the de-waxed bamboo was determined to be 23 % via NREL method (determination of acid-insoluble lignin in biomass). The de-waxed sample was then dried at 60°C in an oven for 16 h prior to ball milling with a planetary ball mill (FritschGMBH, Idar-Oberstein, Germany) for 5 h. The milling bowl was composed of zirconium dioxide (500 ml) and contained 25 zirconium dioxide balls (1 cm diameter). The milling was conducted at room temperature under N_2 atmosphere with a milling frequency of 500 rpm. To prevent overheating, 10-min breaks were followed by 10 min of ball milling. MWL, which represents the native lignin released by aqueous dioxane (96 %, v/v), was prepared according to the classical procedure [15].

Dissolution and Acetylation of Bamboo Meal in DMSO/NMI

Dissolution and acetylation of bamboo cell walls was conducted according to a previous paper [7]. DMSO (10 ml) and NMI (5 ml) (v/v , 2:1) were placed in a round-bottomed flask (50 ml), then the ball-milled bamboo or regenerative one (1 g) was added slowly to the round-bottomed flask, and the mixture was stirred (600 rpm, IKA® RCT basic, Germany) at room temperature to form a homogeneous solution (6 h, forming a brown but clear solution). Subsequently, the dissolved bamboo meal acetylated in situ with 2 ml pyridine-acetic anhydride (1:1, v/v) for 3 h at room temperature under the exclusion of sunlight. The solution turns dark after addition of pyridine-acetic anhydride. After the reaction finished, the acetylated cell walls were regenerated by simply dropping them into distilled water under rapid agitation (2,000 ml of deionized water). The obtained white solid materials were filtered, washed with distilled water, followed by lyophilization. The purified acetylated samples (Ac-B, Ac-RB) were obtained.

Successive Treatments of Ball-Milled Bamboo

The detailed procedures for handling the ball-milled bamboo are shown in Fig. 1. The ball-milled bamboo was treated by two routes described as follows: (1) the ball-milled bamboo cell wall (B) regenerated from DMSO/NMI system (RB) was treated by cellulase. Specifically, the regenerated residue (5 g) was suspended in acetate buffer (250 ml, pH 4.8). Of cellulase, 4.0 ml (Celluclast 1.5 L) was added and incubated at 50°C for 72 h. After centrifugation, the supernatant was removed, and the obtained residue (REB) was washed with water (200 ml). After lyophilization, the residue (1.13 g) was obtained. The dried residue was divided into two parts: a part (0.6 g) was selected to

isolate RCEL. The other part (R1, shown in Fig. 1) remained for preparing acetylated REB (Ac-REB). The dissolution and acetylation was conducted according to the above-mentioned DMSO/NMI procedures. The RCEL was isolated according to the method reported by Zhang et al. [16]. Specially, the residue was extracted with dioxane/water (96:4, v/v , 15 ml) in the dark (2×24 h). The extracted solution was collected by centrifugation and concentration as well as precipitation. The crude RCEL was freeze-dried. To preserve structural features of the isolated RCEL, no further purification was performed, although some carbohydrates remained in the RCEL. The acetylation of RCEL was performed according to a literature [17], but with a few modifications. One hundred milligrams of RCEL was mixed in 4 ml of a solution of acetic anhydride:pyridine (v/v , 1:1). After stirring for 24 h at room temperature under the exclusion of sunlight, the resulted mixture was concentrated under reduced pressure by adding ethanol for several times. The mixture was dropped slowly into 200 ml of ice water (pH=2.0, measured with an acidometer) to induce acetylated lignin precipitation, and the resulted precipitate was washed with deionized water (3×50 ml). After centrifugation and freeze-drying, Ac-RCEL was obtained. In addition, the residue after RCEL extraction was freeze-dried to produce RREL sample, which was subsequently acetylated in DMSO/NMI mixture to obtain Ac-RREL according to the procedures described above. (2) The original ball-milled bamboo (B) was also treated with cellulase (Celluclast 1.5 L). Subsequent procedures were the same as that of the regenerated ball-milled cell wall described above. In this section, the successively acetylated samples (Ac-EB, Ac-REB, Ac-CEL, Ac-RCEL, Ac-REL, and Ac-RREL) were obtained.

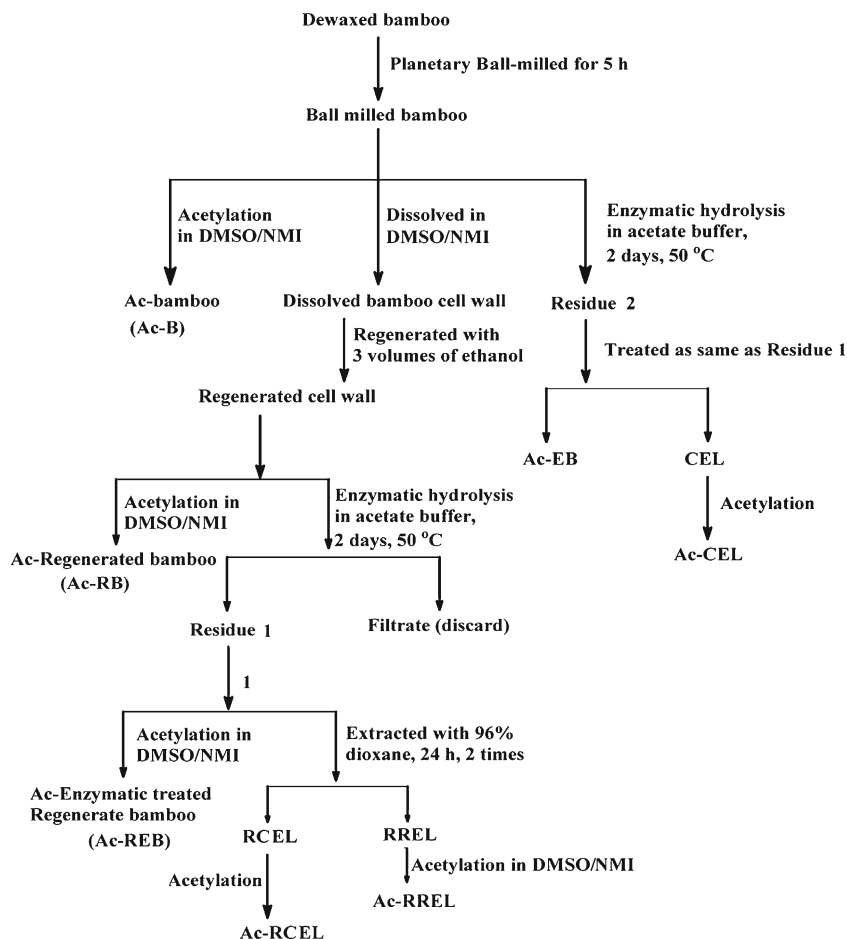
GPC Analyses

The investigation was carried out both on acetylated lignin and on acetylated bamboo samples. Four milligrams of acetylated samples were dissolved in 2 ml tetrahydrofuran (THF), and 20 μl solutions were injected. The weight-average (M_w) and number-average (M_n) molecular weights of the samples were determined by gel permeation chromatography (GPC) on a PL-gel 10 mm Mixed-B 7.5 mm i.d. column, calibrated with PL polystyrene standards according to a previous literature [14]. The analyses were run in duplicate.

FT-IR Analyses

FT-IR spectra of lignin fractions were conducted using a Thermo Scientific Nicolet iN10 FT-IR Microscope (Thermo Nicolet Corporation, Madison, WI, USA) equipped with a liquid nitrogen cooled MCT detector. The dried samples

Fig. 1 Scheme for in situ characterization of bamboo during successive treatments



were ground and palletized using BaF₂, and their spectra were recorded in the range from 4,000 to 700 cm⁻¹ at 4 cm⁻¹ resolution and 128 scans per sample. The fingerprint region was baseline corrected between 1,900 and 750 cm⁻¹. Before data collection, a background scanning was performed for background correction.

NMR Spectra of Acetylated and Non-acetylated Bamboo Samples

Quantitative HSQC (Q-HSQC) NMR spectra were recorded on a 400-MHz NMR spectrometer (Avance III, Bruker, Germany) with a 5-mm BBO probe at 300 K according to the literature with minor modifications [18]. The Bruker standard pulse program hsqcetpsi2 was used for HSQC experiments with some parametric modification. Typically, spectral widths were 4,000 and 20,124 Hz for the ¹H and ¹³C dimensions, respectively. The number of collected complex points was 1,024 for the ¹H dimension with a recycle delay (*d*₁) of 5 s, number of transients for the HSQC spectra was 64, and 256 time increments were always recorded in the ¹³C dimension resulting in an overall experiment time of 22 h. The ¹J_{C-H} used was 150 Hz. Prior to Fourier transformation, the data matrixes were zero filled up to 1,024 points

in the ¹³C dimension. Data processing was performed using standard Bruker's Topspin NMR software. Sixty milligrams of acetylated samples (Ac-B, Ac-RB, Ac-REB, Ac-RCEL, and Ac-RREL) were dissolved in 0.5 ml of CDCl₃, while 60 mg of non-acetylated samples (EB and REB) was dissolved in 0.5 ml of DMSO-*d*₆. Then, the dissolved samples were carefully transferred to NMR sample tubes. Processing used typical matched Gaussian apodization in F2 and a squared cosine-bell in F1 (LB=-0.5, GB=0.001) prior to 2D Fourier transformation. Interactive integrations of contours in 2D HSQC plots were carried out using Bruker's Topspin 2.1 software, as was all data processing.

Results and Discussion

The flowchart and schematic diagram of successive treatments are illustrated in Figs. 1 and 2, respectively. The purpose of this work was to unmask the structural changes of lignin polymer in biomass (grass and bamboo) during the regeneration and enzymatic hydrolysis. During the processes, lignin-rich residues were obtained. Whether the structural features of lignin changed in the residues prompt us to investigate the inhomogeneity of the lignin polymer in the

residue. More importantly, in the current bioethanol production, the structural features of enzymatic hydrolysis residue (EB and REB) should be clarified prior to subsequent utilization.

GPC Analyses of the Bamboo Samples

In order to investigate the changes of the average molecular weight of the bamboo samples during successive treatments, the effects of such treatments on the molecular weight distributions of ball-milled bamboo were firstly evaluated by GPC analyses (Table 1 and Fig. 3). The weight-average molecular weight (M_w) of ball-milled bamboo (B) slightly decreased after being regenerated from the DMSO/NMI mixture (RB). However, the enzymatic treatments of ball-milled bamboo (B) and the regenerative bamboo (RB) resulted in a higher M_w of REB than that of EB. The lower M_w of RB was probably due to the slight depolymerization of the ball-milled bamboo during the regeneration process in the initial step, while the higher M_w of REB suggested that more carbohydrates, which probably have a small M_w , could be easily hydrolyzed. Additionally, the fact that a portion of small lignin fragments caused by ball-milling were removed after the DMSO/NMI regeneration process [19] would add some clues to explain the higher M_w of REB. Table 1 also shows the GPC results of the original bamboo (B and RB) and the treated bamboo (EB and REB). It was found that a significant decrease occurred in the molecular weight of enzymatic treated bamboo (EB, REB), which was mostly related to the hydrolysis of carbohydrates.

The dissolution or swelling of cellulose by solvents was considered to be a more facile method for disrupting the crystalline structure to increase its accessibility to cellulases [16, 20]. After the treatment with cellulast 1.5 L, it was found that the mass losses for original and regenerated ball-milled bamboo were 70 % and 78 %, respectively. It is therefore possible to deduce that the regeneration has been shown to be effective to produce a highly digestible cellulose-rich residue.

The molecular weights of REL and CEL from ball-milled bamboo were found to be higher than those from regenerated bamboo samples (RREL and RCEL). It has been reported that the carbohydrate polymer linked to lignin can increase the hydrodynamic volume of lignin and therefore increase the apparent molar mass of the lignin when it is measured using GPC [21]. Take the fact that the RREL and RCEL from the regenerated bamboo contained less carbohydrate into consideration, therefore, the lower molecular weights of RREL and RCEL were not surprised.

FT-IR Spectra of the Treated Bamboo Samples

FT-IR was used to briefly investigate the changes of bamboo during the various treatments. Figure 4 shows the FT-IR spectra of the treated ball-milled bamboo preparations (acetylated samples). It was found that the O–H stretching vibration at $3,430\text{ cm}^{-1}$ sharply decreased as compared to the original ball-milled bamboo (not shown). However, a small absorption centered at $3,458\text{ cm}^{-1}$ was still existent due to

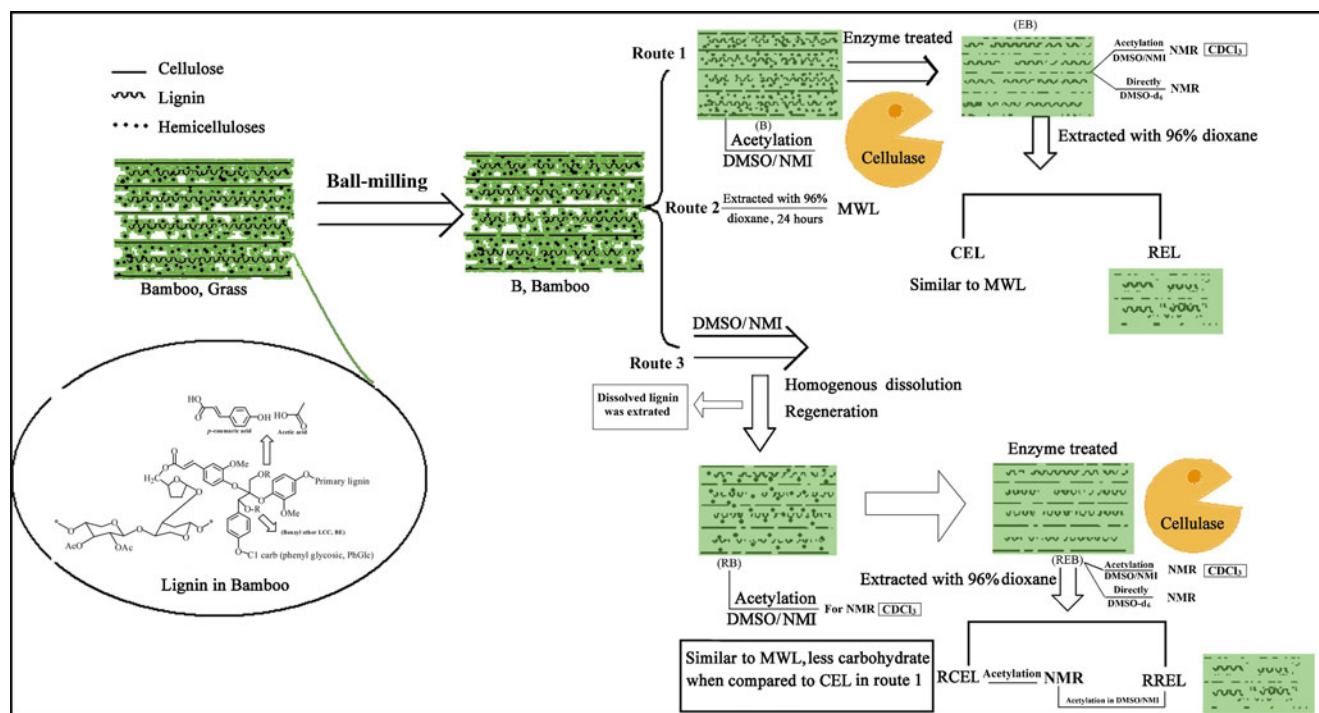


Fig. 2 The proposed evolutionary mechanism of bamboo cell wall during the chemical and enzymatic treatments

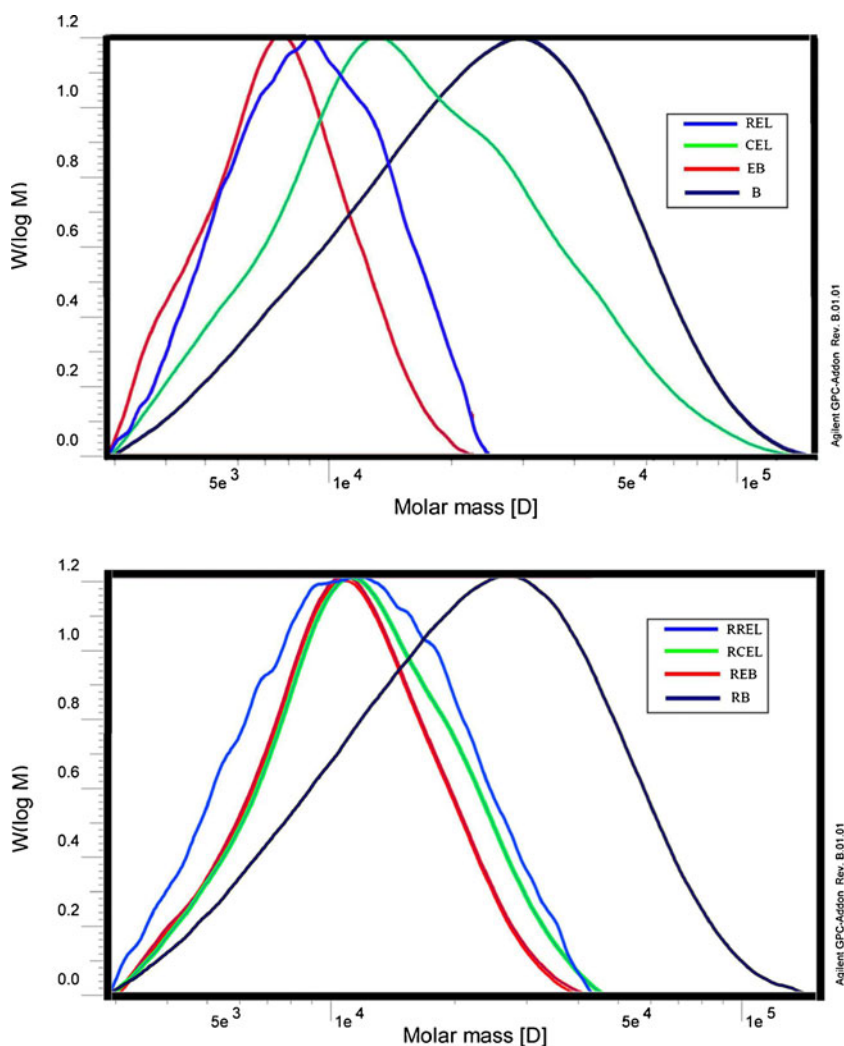
Table 1 Weight-average (M_w) and number-average (M_n) molecular weights of the successively treated bamboo preparations

Samples	B	RB	EB	REB	REL	RREL	CEL	RCEL
M_w	29,510	27,670	7,500	8,160	10,480	10,010	13,780	9,300
M_n	17,310	16,450	4,520	5,210	8,540	8,090	6,200	5,660
M_w/M_n	1.70	1.67	1.66	1.56	1.22	1.23	2.22	1.64

the residual OH stretching after acetylation. A previous report demonstrated that the absorption represented for OH groups cannot be totally eliminated even though the reaction was conducted in ionic liquid (ILs), and the reagent was extremely slowly added to the reaction system [22]. In addition, the larger absorption at 1,749 cm^{-1} that appeared in all the bamboo samples indicated that acetylation successfully occurred. The strong band at 1,041 cm^{-1} is assigned to C–O stretching in cellulose, hemicelluloses, and lignin or C–O–C stretching in cellulose and hemicelluloses (B and RB) [23]. However, the absorption is sharply decreased in other samples (EB, REB, CEL, RCEL, REL, and RREL). Simultaneously, the signals represent for lignin polymer, which appear at 1,597, 1,506, and 1,426 cm^{-1} (aromatic skeletal

vibrations); 1,325 cm^{-1} (syringyl and condensed guaiacyl); 1,163 cm^{-1} (HGS lignin); 1,125 cm^{-1} (GS lignin); and 832 cm^{-1} (C–H out-of-plane in H units), increased in the samples EB, REB, CEL, and RCEL [24]. The increasing signals for lignin suggest that most of the carbohydrates were degraded (cellulose and hemicelluloses) after the enzymatic treatment. Besides, it should be noted that the samples of REL and RREL, which are the residues after CEL extractions, still contained a portion of lignin in it, as shown in FT-IR spectra. Furthermore, the sharp band at 899 cm^{-1} , which is originated from the β -glucosidic linkages between the monosaccharide units in hemicelluloses and cellulose, is also decreased after cellulase hydrolysis. This further implied the degradation of β -glucosidic linkages carbohydrates (cellulose and xylans). In

Fig. 3 GPC profiles of the successively treated bamboo samples



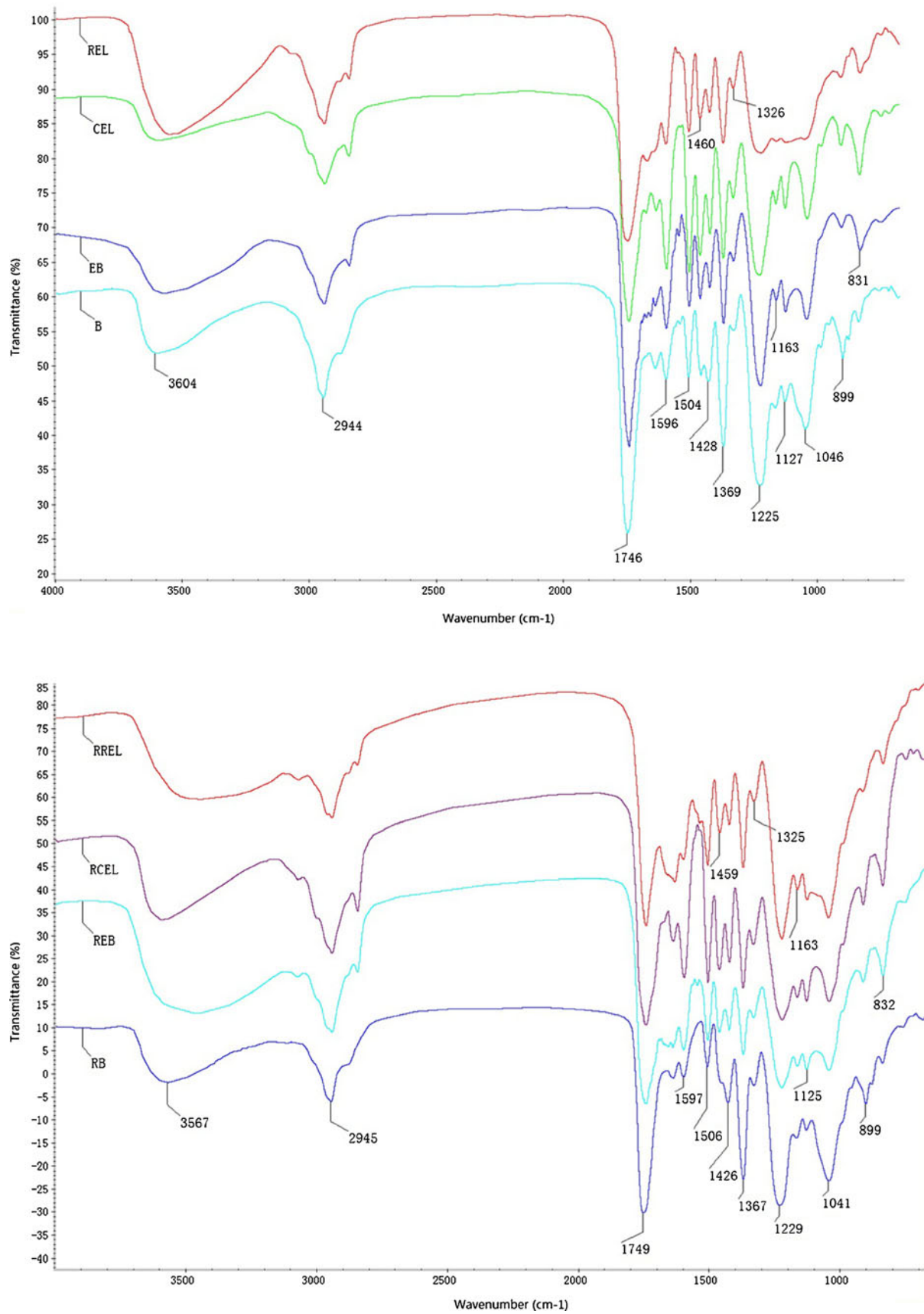


Fig. 4 FT-IR spectra of the acetylated bamboo samples

brief, FT-IR spectra give less information about the compositional changes of bamboo during the regeneration and enzymatic treatment. However, the brief understanding of the treated samples, such as the lignin type (HGS type) and the degradation of carbohydrate, could be obviously attained.

Structural Changes of Carbohydrates in the Acetylated Bamboo Samples during Various Treatments

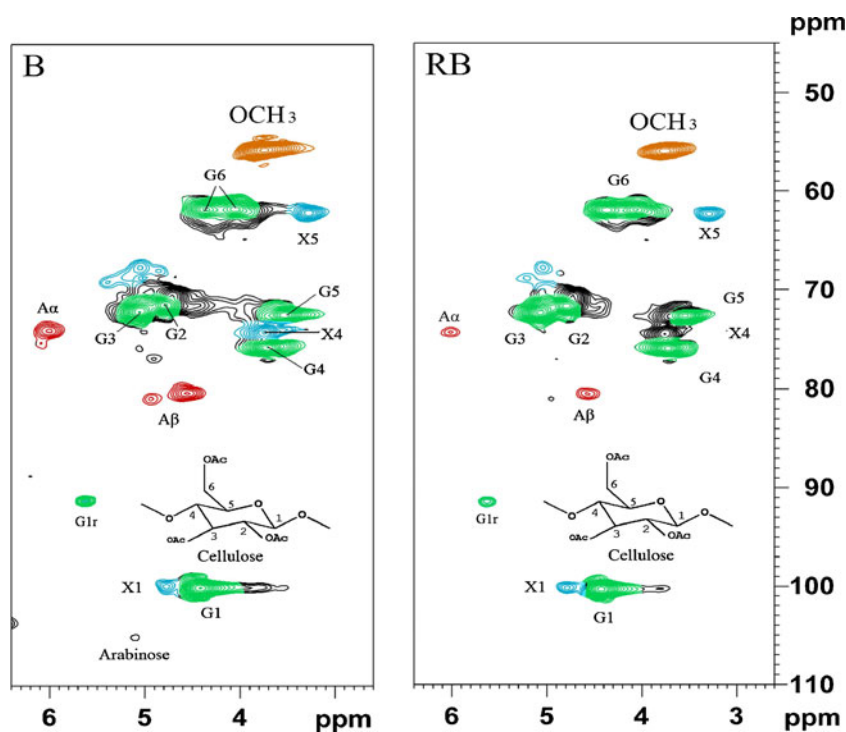
To detect the structural changes of carbohydrate in the treated bamboo samples, the acetylated samples were analyzed with 2D ^1H - ^{13}C HSQC NMR (Figs. 5, 6 and 7). Figure 5 gives the HSQC spectra of ball-milled bamboo and regenerated ball-milled bamboo. It was also observed that the carbohydrates in the bamboo samples changed slightly before (B) and after regenerated (RB) treatment. A previous study indicated that a portion of dissociative lignin rather than carbohydrates could be isolated from plant cell wall via regeneration process [19]. However, the signals represented for cellulose were distinctly observed at a higher contour level. The correlations of $\text{C}_1\text{-H}_1$ (Glc₁), $\text{C}_2\text{-H}_2$ (Glc₂), $\text{C}_3\text{-H}_3$ (Glc₃), $\text{C}_4\text{-H}_4$ (Glc₄), $\text{C}_5\text{-H}_5$ (Glc₅), and $\text{C}_6\text{-H}_6$ (Glc₆) in the acetylated cellulose were observed at $\delta_{\text{C}}/\delta_{\text{H}}$ 101.1/4.40, 71.5/4.77, 72.1/5.05, 75.7/3.70, 72.5/3.53, 61.76/4.34, and 61.76/4.04 ppm, which was in agreement with previous literatures [7, 25]. The $\text{C}_1\text{-H}_1$ correlation of xylan was probably overlapped with that of cellulose and gives an overlapped signal at about $\delta_{\text{C}}/\delta_{\text{H}}$ 101.1/4.4 ppm. By contrast, the $\text{C}_1\text{-H}_1$ of $\alpha\text{-L-Araf}$ unit in the bamboo cell wall was expressly observed at $\delta_{\text{C}}/\delta_{\text{H}}$ 105.5/

5.15 ppm [11]. These results were in line with the previous results that arabinoxylan comprised more than 90 % of bamboo hemicelluloses [26]. Besides, an evident signal at $\delta_{\text{C}}/\delta_{\text{H}}$ 91.8/5.64 ppm was assigned to reducing ends of (1-4)- $\alpha\text{-D-Glc}$ according to previous reports [11, 25]. After treatment with cellulase, it was found that some signals for carbohydrate still appeared in REB, RCEL, and RREL, suggesting the carbohydrate cannot be hydrolyzed completely under the conditions given. However, the signals for 4-*O*-methyl- $\alpha\text{-D-glucuronic}$ acid unit, which is one of the side chains in xylan from grass species, were not found [27]. The potential reason for this could be attributed to the esterase activity of cellulase [28]. Furthermore, although the ball-milled bamboo is treated with regeneration and enzymatic hydrolysis, varying signals from the associated carbohydrates could also be found in the HSQC spectra of REB and RCEL, even in the final residue (RREL). However, the associated carbohydrates observed herein give us an inspiration to investigate the LCC of the bamboo samples in subsequent sections.

Structural Analysis of Lignin in the Acetylated Bamboo Samples during Various Treatments

2D ^1H - ^{13}C HSQC NMR spectra were used to track the structure heterogeneity of the lignin in the treated bamboo samples by simple acetylation in DMSO/NMI mixture in this study. Figure 6 shows the HSQC spectra (side chain region) of the acetylated bamboo samples (RB, REB, RREL, and RCEL). The HSQC spectra of acetylated cell

Fig. 5 HSQC of cellulose component in the ball-milled bamboo and regenerated ball-milled bamboo (acetylated)



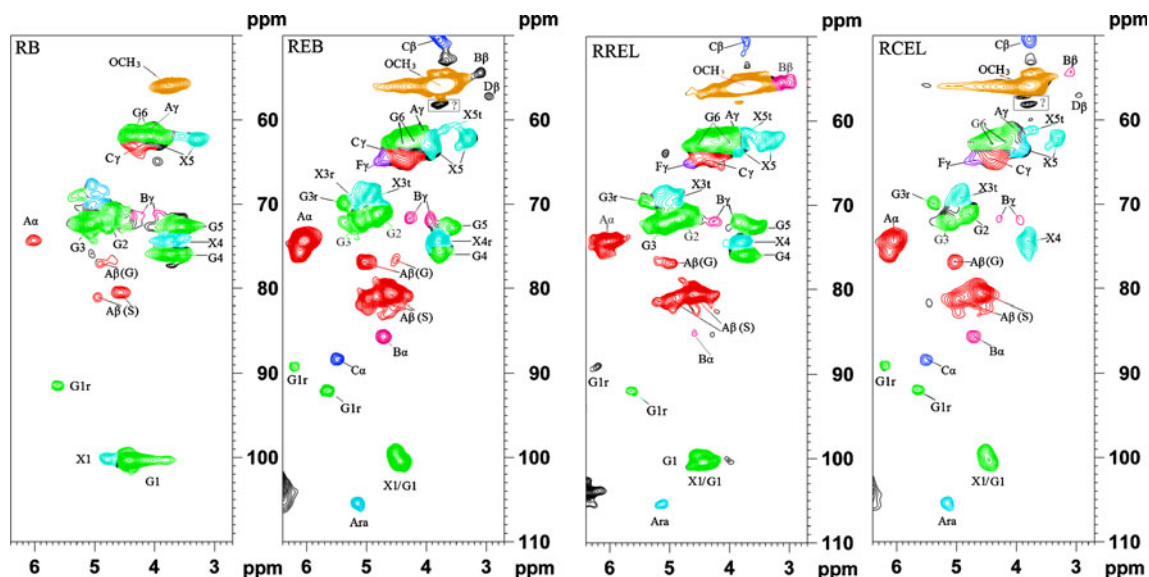


Fig. 6 The side chain region of HSQC spectra in the treated bamboo samples (acetylated)

walls (softwood and hardwood) have been obtained by the equal dissolved system [7]. However, only the signals for cellulose and aromatic region of lignin polymer were obviously distinguished. The side chain region of lignin was still overlapped with numerous signals of carbohydrate, which was deemed to impede the in situ characterization of lignin by NMR techniques. In this study, the successively treated samples were used to unmask the structural heterogeneity of lignin in bamboo via in situ method. It was found that the samples (B and RB) show distinct signals for β -O-4 (A)

and methoxy group (OMe). However, other inter-linkages signals, such as β - β (B), β -5 (C), and β -1 (D), are overlapped with other signals for carbohydrates. After enzymatic hydrolysis, REB shows the unequivocal signals of lignin, especially the distinguishable side chain of spectra as compared to that of RB (Fig. 6). However, the spectra of EB and REB were found to be similar except for different abundances. The CEL preparations extracted from the original and regenerated ball-milled bamboo were also used for characterization of lignin polymer. However, the CEL obtained

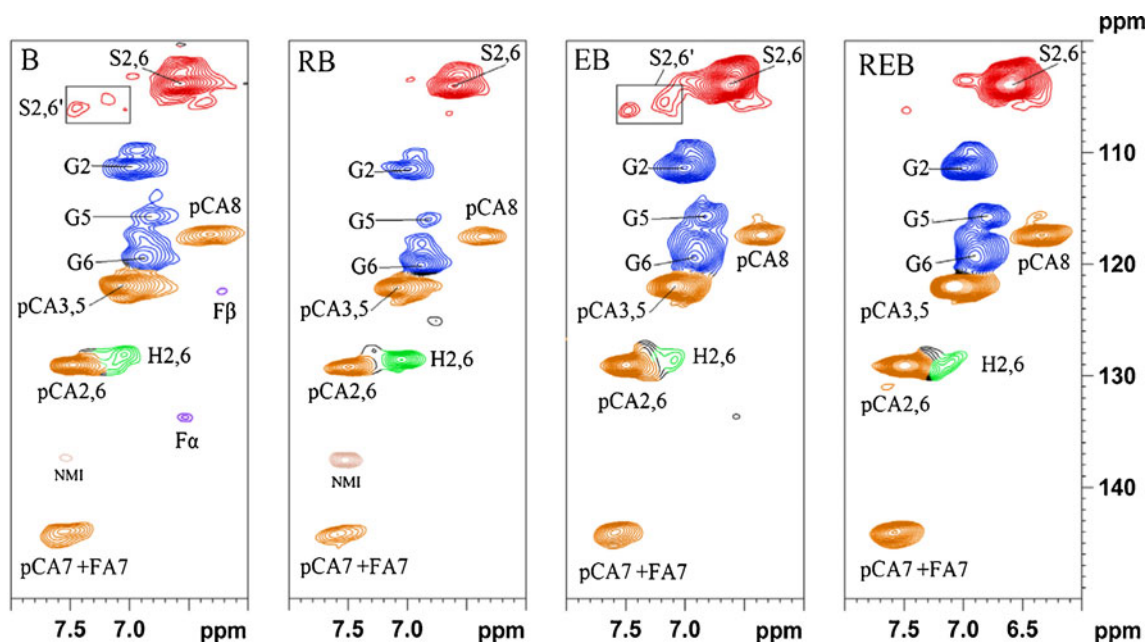


Fig. 7 The aromatic regions of HSQC spectra of the acetylated samples

based on DMSO/NMI regenerated system (i.e., RCEL) was only used for structural analysis since a previous study has demonstrated that the CEL from original and regenerated ball-milled wood presented a similar structure feature, just differed in the yield [16]. In addition, the final residue REL (i.e. RREL) after RCEL extraction, which rarely been used for structural analysis of lignin via liquid NMR technique due to its limited solubility, was also investigated by 2D HSQC NMR via acetylating the residue in DMSO/NMI dissolving system. Furthermore, more distinct signals for lignin polymer were found in the order of RB<REB<RCEL. However, RREL was observed to contain less lignin polymer since the lignin exposed after enzymatic hydrolysis was mostly separated as RCEL by 96 % aqueous dioxane.

The distinguishability of the spectra was significantly improved after enzymatic hydrolysis of RB. It was found that REB shows a similar spectrum to that of RCEL (Fig. 6). Therefore, the REB was selected to illustrate the lignin structure in this study. The C–H correlations from all major lignin substructures (β -O-4, β - β , β -5, and β -1) can be readily assigned. The prominent correlating signals observed are the methoxyl groups (OMe, δ_C/δ_H 55.6/3.76 ppm) and β -O-4 aryl ether linkages. The C_α - H_α correlation in β -O-4 substructures (A) was observed at δ_C/δ_H 74.1/6.02 ppm. The signals located at δ_C/δ_H 76.6/5.07 and 80.3/4.59 ppm are attributed to the G-type and S-type of β -O-4 (β -position), respectively [16]. The C_γ - H_γ correlation of β -O-4 structure was probably at about δ_C/δ_H 61.0–63.0/4.19–4.4 ppm, which is seriously overlapped with Glc6 correlating signals. In addition, the C_γ - H_γ of acylated β -O-4 was not clearly observed. The C_α - H_α , C_β - H_β , and C_γ - H_γ correlations of the resinol B (β - β) substructures appeared at δ_C/δ_H 85.6/4.70, 71.7/3.92–4.28, and 54.3/3.08 ppm, respectively [16]. The correlations at $\delta_C/$

δ_H 88.2/5.49 and 50.2/3.77 ppm are originated from the C_α - H_α and C_β - H_β of the phenylcoumaran C (β -5) structures. However, their C_γ - H_γ correlations were overlapped with other signals. In addition to these linkages, the C_α - H_α , C_β - H_β , and C_γ - H_γ correlations (δ_C/δ_H 133.0/6.60, 123.0/6.30, and 64.2/4.7 ppm) in *p*-hydroxycinnamyl alcohol end groups (F) and the C_β - H_β correlation (δ_C/δ_H 57.5/2.98 ppm) of spirodienone substructure (D) were also tentatively assigned [11]. Even in the residue (RREL), the main substructures, such as β -O-4, β - β , and β -5, and *p*-hydroxycinnamyl alcohol end groups could also be assigned (A, B, C, and F unit, depicted in Fig. 11). Therefore, the data presented in the spectra suggest that the structure of RREL was similar to those of native lignin. However, the RREL was not easily dissolved in DMSO due to the association with carbohydrates, which was in agreement with a previous study [8].

In the aromatic regions of the HSQC spectra of different acetylated bamboo samples (B, RB, EB, REB, RREL, and RCEL, shown in Figs. 7 and 8), cross-signals from syringyl (S), guaiacyl (G), and *p*-hydroxyphenyl (H) lignin units could be distinctly observed. The S-type lignin units showed a prominent signal for the $C_{2,6}$ - $H_{2,6}$ correlations at δ_C/δ_H 104.1/6.59 ppm, whereas the G-type lignin showed different correlations for C_2 - H_2 , C_5 - H_5 , and C_6 - H_6 at δ_C/δ_H 110.7/6.96, 116.0/6.80, and 120.1/6.87 ppm, respectively. Signals corresponding to $C_{2,6}$ - $H_{2,6}$ correlations in C_α -oxidized S units (δ_C/δ_H 105.7/7.17 and 106.1/7.47 ppm) are presented in the HSQC spectra (B, EB, REB, and RCEL), but were not found in the spectra of RB and RREL. This fact suggested that the oxidized lignin fractions derived from ball milling was extracted in the initial regeneration process (Fig. 2, Route 3). However, some oxidized lignin fractions were probably released after enzymatic hydrolysis process, as

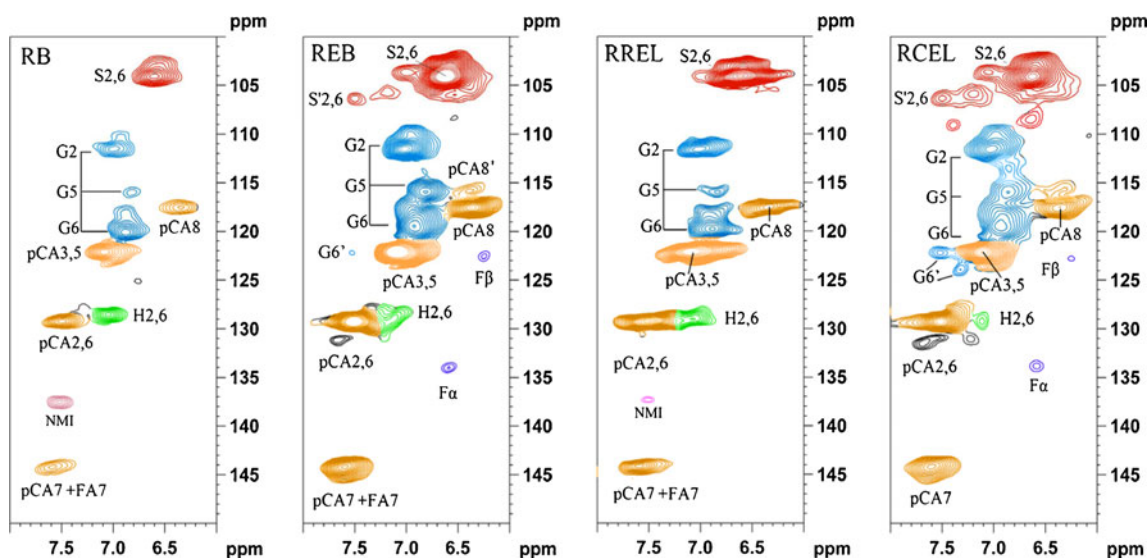


Fig. 8 The aromatic regions of HSQC spectra of the treated bamboo samples (acetylated)

shown in REB and RCEL (Fig. 8). The correlations for the C₆–H₆ in oxidized α -ketone structures **G'** was tentatively assigned in the spectrum of RCEL. Furthermore, the C_{2,6}–H_{2,6} aromatic correlating signals from **H** units were clearly observed at δ_C/δ_H 128.8/7.05 ppm.

A previous report indicated that *p*-coumaric acid (**pCA**) is acylated at C- γ of lignin side chain in grass species [29]. To clarify the existence of the acylated **pCA** in the bamboo samples, the HSQC spectra of in vitro acetylated bamboo samples were investigated in detail. The **pCA**_{2/6} correlations in the acetylated bamboo samples are found at δ_C/δ_H 129.3/7.48 ppm, and **pCA**_{3/5} correlations at δ_C/δ_H 122.0/7.08 ppm. However, the **pCA**_{3/5} and **pCA**_{2/6} correlations were found at δ_C/δ_H 115.8/6.83 and 130.2/7.48 ppm in non-acetylated bamboo cell walls. The **pCA**₈ gave a correlation at δ_C/δ_H 117.4/6.33 ppm, while the corresponding signal in the non-acetylated samples was found at δ_C/δ_H 113.9/6.29 ppm [3]. In consideration of the migration of chemical shifts value (δ) of the correlative signals of **p-CA**_{3/5} and **p-CA**₈ to low field (high δ value) after acetylation, therefore, the in vitro acetylation was demonstrated to occur at C-4 of **p-CA**. Besides, the question that whether the **p-CA** acylated at C- γ of lignin still remain uncertain from the spectra. Adding the accessional evidence of the subsequent HSQC spectra of non-acetylated bamboo samples, the analysis suggested that the in vitro acetylation occurred at C-4 (phenolic hydroxyl group) of **p-CA**. In addition, **p-CA** was esterified to the C- γ of the side chain of lignin in the evolutionary process of the bamboo.

Structural Analysis of Lignin in the Non-acetylated Bamboo Samples during Various Treatments

Chemical modification of the cell wall, even simple derivatization, leads to the loss of some information. For example, natural acetylation in the wall is masked when the sample is per-acetylated. To detect the possible changes of the bamboo samples after in vitro acetylation with acetic anhydride in DMSO/NMI system, the enzymatic-treated bamboo samples (EB and REB) were subsequently examined by NMR without derivatization. Fortunately, the EB and REB were found to be entirely dissolved in DMSO-*d*₆ under ordinary ultrasonic bath for a few hours. Figure 9 shows the HSQC spectra of the RB and REB as well as MWL.

Aliphatic Regions

In general, few reports discuss the aliphatic region of HSQC spectra due to the insufficiency of structural information. In this study, the aliphatic region of the acetylated and non-acetylated bamboo samples was subjected to investigation (not shown). In the samples of Ac-B and Ac-RB, acetate

peaks at about δ_C/δ_H 20.3/2.00 ppm were found. However, two peaks at δ_C/δ_H 20.4/2.00 and 20.6/2.27 ppm in the spectra of Ac-EB and Ac-REB were observed. It is well known that polysaccharide contours are logically dominant because they are whole plant cell wall samples (Ac-B and Ac-RB). Therefore, the intense signals at δ_C/δ_H 20.3/2.00 ppm were likely attributed to the acetylated polysaccharides (hemicelluloses and cellulose), while the signals at δ_C/δ_H 20.6/2.27 ppm were probably due to the acetylated lignin polymer (acetyl groups occurred at Ar-OH of lignin) [17]. In addition, in the non-acetylated bamboo samples EB and REB, the acetate peak appeared at δ_C/δ_H 20.4/1.90 ppm. In view of the absence of 2-*O*-Ac- β -D-Xylp correlation at δ_C/δ_H 73.5/4.64 ppm and 3-*O*-Ac- β -D-Xylp correlation at δ_C/δ_H 75.0/4.94 ppm in the spectra of EB and REB, the acetates peaks that appeared in non-acetylated samples (EB and REB) were likely assigned to in vivo acetylated lignin polymer. Actually, Ralph and Lu have confirmed acetates in lignins to be unambiguously detected and confirm their presence at the γ -positions of lignin side chains in grass species [30].

Lignin Side Chain Regions

In this section, the two non-acetylated samples (EB and REB) and MWL were directly dissolved in DMSO-*d*₆ to investigate the structural features of lignin polymers. It was found that they provide remarkably well resolved spectra that can be compared to that of MWL in the present study (Fig. 9). The important correlations, such as those from substructures of β -ether (β -O-4) **A**, resinol (β - β) **B**, and phenylcoumaran (β -5) **C** can be readily assigned according to the recent literatures [3, 12, 13]. Interestingly, oxidized substructure β -ether (β -O-4) **A''** was also found in the spectra of MWL and EB rather than REB according to previous reports [31, 32]. The fact that oxidized substructures appeared in the initial extraction and treated sample were in agreement with the acetylated samples that were discussed in the aforementioned.

Specially, the correlations for γ -position of substructure **A** could be seen at δ_C/δ_H 59.9/3.35–3.80 ppm, while its γ -acylated β -ether units **A'** (γ -**pCA** or γ -Ac) were clearly seen at δ_C/δ_H 63.4/4.42 and 63.4/3.94 ppm, but the correlation at δ_C/δ_H 63.4/3.94 ppm are overlapped with one of the 5-position peaks of xylans [27]. Moreover, the other signals assigned to xylans were evidently identified, with its C₄–H₄, C₃–H₃, and C₂–H₂ correlations (**X**₄, **X**₃, and **X**₂) at δ_C/δ_H 75.3/3.56, 73.6/3.25, and 72.5/3.05 ppm, respectively (Table 2). It has been reported that the spectra of corn cell wall showed a strong 2-*O*-Ac- β -D-Xylp C₂–H₂ correlation at δ_C/δ_H 73.5/4.64 ppm and a 3-*O*-Ac- β -D-Xylp C₃–H₃ correlation at δ_C/δ_H 75.0/4.94 ppm [3]. However, the xylans-attached acetyl groups were not found in the spectra

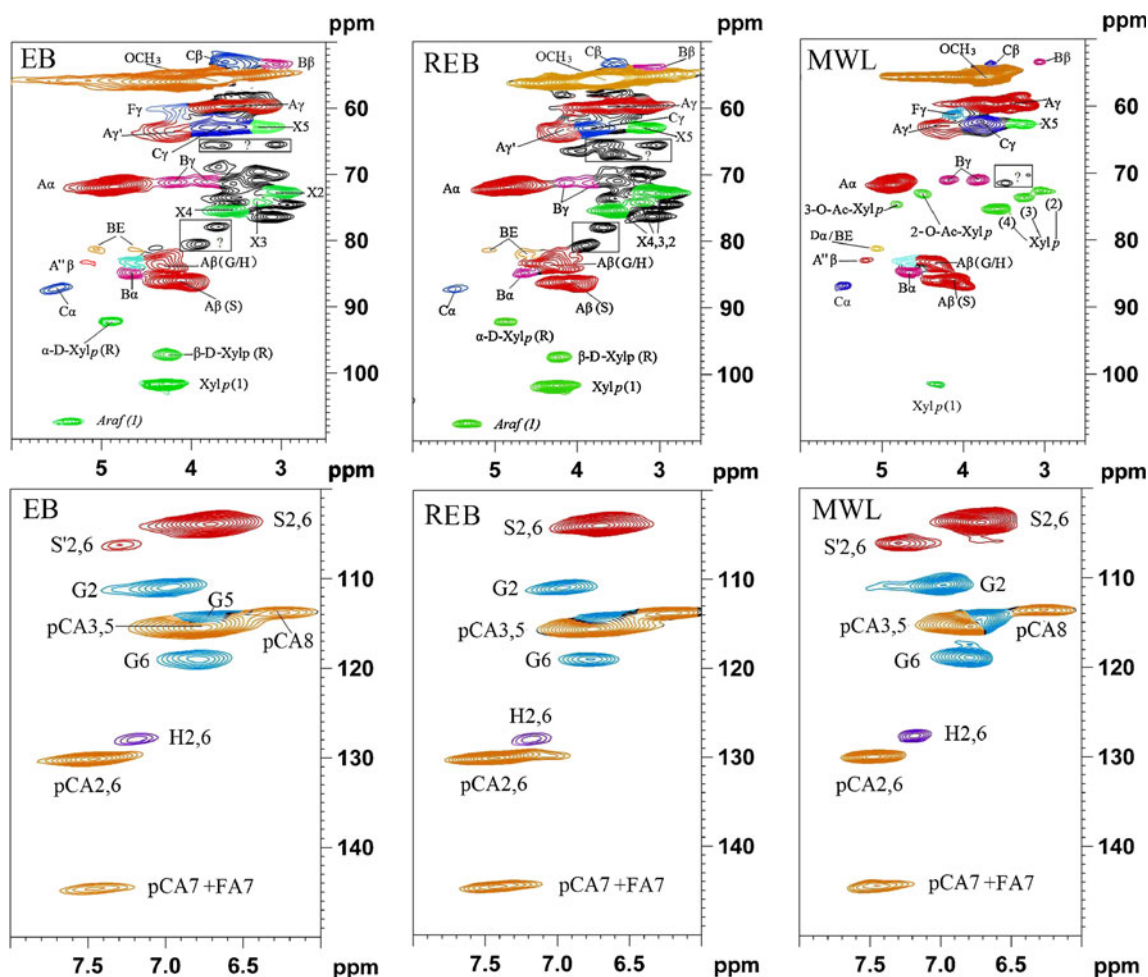


Fig. 9 HSQC spectra of EB, REB, and MWL (non-acetylated)

of enzyme-treated residues (EB and REB) but that appeared in the MWL from the same starting materials (ball-milled bamboo). This suggested that the acetyl groups in acetylated xylans were probably degraded during the enzymatic hydrolysis. Coincidentally, a previous report also found that the cellulase preparation might also possess esterase activity [28].

Aromatic Region

The syringyl–guaiacyl composition of bamboo lignins is clearly evidenced in the aromatic region of these in situ NMR spectra (Fig. 9). Specially, a significant correlation for the syringyl units (S) was observed at δ_C/δ_H 103.8/6.69 ppm; while its oxidized (α -ketone) structures S' appeared at δ_C/δ_H 106.2/7.28 ppm in EB and MWL rather than REB, it was not yet clear to realize what degree this oxidation occurs in the lignification process in the plant vs. in the procedure of sample preparation (ball milling, enzymatic hydrolysis, and derivatization in the DMSO/NMI system). With the exception of S units, all of the guaiacyl

components which are in the lignin of the EB and REB can be expressly distinguished. The correlation for the G₂ position is at δ_C/δ_H 110.7/6.96 ppm. However, the fact that the correlations of G'₂ and S'_{2,6} were not found in non-acetylated REB suggested that the oxidized lignin fragments originated from ball-milled process were removed after the regenerative process. This was somewhat inconsistent with the above-mentioned acetylated bamboo samples (Ac-RCEL and Ac-REB) since oxidized lignin was also found in the HSQC spectra of these samples. The fact suggested that oxidation probably occurred during acetylating process. However, this result needs further verification. In addition, the C–H correlations of G₅ were observed at δ_C/δ_H 114.8/6.71 ppm, and most of the G₆ correlations were located at δ_C/δ_H 118.8/6.77 ppm, minor oxidized G'₆ also occasionally occurred at higher chemical shifts value (δ_C/δ_H 122.6/7.54 ppm) [3].

The question that whether the pCA acylated to C- γ of lignin in the enzymatic-treated bamboo samples was clarified by the chemical shifts of pCA₈ in the non-acetylated bamboo samples (EB, REB, and MWL). It was observed

Table 2 The NMR assignments of major components in the HSQC spectra of the bamboo samples

Label	δ_C/δ_H (ppm) ^a	δ_C/δ_H (ppm) ^b	Assignments
C $_{\beta}$	53.1/3.46	50.2/3.77	C $_{\beta}$ -H $_{\beta}$ in phenylcoumaran (C)
B $_{\beta}$	53.5/3.07	54.3/3.08	C $_{\beta}$ -H $_{\beta}$ in β - β (resinol) (B)
OMe	56.4/3.70	55.6/3.76	C-H in methoxyls (OMe)
D $_{\beta}$	ND	57.5/2.98	C $_{\beta}$ -H $_{\beta}$ in spirodienone substructure (D)
A $_{\gamma}$	59.9/3.35	62.53/4.40	C $_{\gamma}$ -H $_{\gamma}$ in β -O-4 substructures (A)
A $_{\gamma}$	59.9/3.80	62.53/4.19	C $_{\gamma}$ -H $_{\gamma}$ in β -O-4 substructures (A)
A $_{\gamma'}$	63.4/4.16	64.0/4.70	C $_{\gamma}$ -H $_{\gamma}$ in γ -acylated β -O-4 (A')
F $_{\gamma'}$	61.4/4.10	64.2/4.70	C $_{\gamma}$ -H $_{\gamma}$ in <i>p</i> -hydroxycinnamyl alcohol (F)
B $_{\gamma}$	71.8/3.81	71.7/3.92	C $_{\gamma}$ -H $_{\gamma}$ in β - β resinol (B)
B $_{\gamma}$	71.8/4.17	71.7/4.28	C $_{\gamma}$ -H $_{\gamma}$ in β - β resinol (B)
A $_{\alpha}$	72.0/4.85	74.1/6.02	C $_{\alpha}$ -H $_{\alpha}$ in β -O-4 unit (A)
A $_{\beta(G/H)}$	83.9/4.29	76.6/5.07	C $_{\beta}$ -H $_{\beta}$ in β -O-4 linked to G/H (A)
B $_{\alpha}$	84.7/4.64	85.6/4.70	C $_{\alpha}$ -H $_{\alpha}$ in β - β (resinol) (B)
A $_{\beta(S)}$	85.8/4.10	85.8/4.10	C $_{\beta}$ -H $_{\beta}$ in β -O-4 linked to S (A)
A'' $_{\beta}$	83.1/5.21	ND	C $_{\beta}$ -H $_{\beta}$ in oxidized (C $_{\alpha}$ =O) β -O-4 (A'')
C $_{\alpha}$	87.6/5.50	88.2/5.49	C $_{\alpha}$ -H $_{\alpha}$ in phenylcoumaran (C)
D $_{\alpha}$	81.2/5.09 ^c	ND	C $_{\alpha}$ -H $_{\alpha}$ in spirodienone substructure (D)
S $_{2,6}$	103.7/6.69	104.1/6.59	C $_{2,6}$ -H $_{2,6}$ in syringyl units (S)
S' $_{2,6}$	106.1/7.28	105.7/7.17	C $_{2,6}$ -H $_{2,6}$ in oxidized S units (S')
F $_{\beta}$	128.2/6.25	123.0/6.30	C $_{\beta}$ -H $_{\beta}$ in <i>p</i> -hydroxycinnamyl alcohol (F)
F $_{\alpha}$	128.2/6.44	133.0/6.60	C $_{\alpha}$ -H $_{\alpha}$ in <i>p</i> -hydroxycinnamyl alcohol (F)
G $_{5}$	114.8/6.71	116.0/6.80	C $_{5}$ -H $_{5}$ in guaiacyl units (G)
G $_{6}$	118.8/6.77	120.1/6.87	C $_{6}$ -H $_{6}$ in guaiacyl units (G)
H $_{2,6}$	127.8/7.17	128.8/7.05	C $_{2,6}$ -H $_{2,6}$ in H units (H)
X $_{1}$	101.5/4.25	101.1/4.70	C $_{1}$ -H $_{1}$ in β -D-xylopyranoside
X $_{2}$	72.5/3.05	ND	C $_{2}$ -H $_{2}$ in β -D-xylopyranoside
X' $_{2}$	73.5/4.52	ND	2-O-Ac- β -D-xylopyranoside (MWL)
X $_{3}$	73.6/3.25	ND	C $_{3}$ -H $_{3}$ in β -D-xylopyranoside
X' $_{3}$	75.0/4.94	ND	3-O-Ac- β -D-xylopyranoside (MWL)
X $_{4}$	75.3/3.56	ND	C $_{4}$ -H $_{4}$ in β -D-xylopyranoside
X $_{5}$	63.2/3.24	62.5/3.31	C $_{5}$ -H $_{5}$ in β -D-xylopyranoside
X $_{5}$	63.2/3.94	62.5/3.85	C $_{5}$ -H $_{5}$ in β -D-xylopyranoside
BE $_{\alpha}$ (I)	81.3/4.65	ND	C $_{\alpha}$ -H $_{\alpha}$ in benzyl ether LCC (I)
BE $_{\alpha}$ (II)	81.2/5.04	ND	C $_{\alpha}$ -H $_{\alpha}$ in benzyl ether LCC (II)
PhGlc1	99.5/4.90	ND	Phenyl glycoside linkages
PhGlc2	100.0/5.10	ND	Phenyl glycoside linkages

Table 2 (continued)

Label	δ_C/δ_H (ppm) ^a	δ_C/δ_H (ppm) ^b	Assignments
PhGlc3	101.9/4.89	ND	Phenyl glycoside linkages
PCE $_{3,5}$	115.8/6.83	122.0/7.08	C $_{3,5}$ -H $_{3,5}$ in <i>p</i> -coumarate
PCE $_{2,6}$	130.2/7.48	129.3/7.48	C $_{2,6}$ -H $_{2,6}$ in <i>p</i> -coumarate
PCE $_{7}$	144.8/7.51	144.8/7.51	C $_{7}$ -H $_{7}$ in <i>p</i> -coumarate
PCE $_{8}$	113.9/6.29	117.4/6.33	C $_{8}$ -H $_{8}$ in <i>p</i> -coumarate
FA $_{2}$	110.7/7.35	ND	C $_{2}$ -H $_{2}$ in ferulate
FA $_{6}$	123.1/7.17	ND	C $_{6}$ -H $_{6}$ in ferulate
FA $_{7}$	144.8/7.51	ND	C $_{7}$ -H $_{7}$ in ferulate
Glc $_{1}$	ND	100.1/4.4	C $_{1}$ -H $_{1}$ in cellulose
Glc $_{2}$	ND	71.5/4.77	C $_{2}$ -H $_{2}$ in cellulose
Glc $_{3}$	ND	72.1/5.05	C $_{3}$ -H $_{3}$ in cellulose
Glc $_{4}$	ND	75.7/3.70	C $_{4}$ -H $_{4}$ in cellulose
Glc $_{5}$	ND	72.5/3.53	C $_{5}$ -H $_{5}$ in cellulose
Glc $_{6}$	ND	61.76/4.34	C $_{6}$ -H $_{6}$ in cellulose
Glc $_{6}$	ND	61.76/4.04	C $_{6}$ -H $_{6}$ in cellulose

The signal of residual NMI appeared at δ_C/δ_H 137.0/7.50 ppm

ND not detected

^a δ_C/δ_H (ppm), the HSQC spectra assignments of non-acetylated samples

^b δ_C/δ_H (ppm), the HSQC spectra assignments of acetylated samples

^c The signal is probably overlapped with benzyl ether LCC linkage

that the **pCA $_8$** correlations are located at δ_C/δ_H 113.9/6.29 ppm in these samples. In addition, the **pCA $_{2/6}$** correlations are at δ_C/δ_H 130.2/7.48 ppm, and their 3,5-correlations at δ_C/δ_H 115.8/6.83 ppm are overlapped with those from guaiacyl units in these non-acetylated bamboo samples. The **pCA $_7$** correlation (δ_C/δ_H 144.8/7.51) is also noted. The signals observed are highly consistent with the reported NMR data for *p*-coumarate units [3]. In addition to the obvious signals of *p*-coumarate units, minor signals for ferulate (**FA**), which is believed to be responsible for cell wall cross-linking in grasses, are also well resolved. The **FA $_2$** and **FA $_6$** correlations were observed at δ_C/δ_H 110.7/7.35 and 123.1/7.17 ppm (not displayed in the current contour level), respectively. Moreover, **FA $_7$** correlation coincides with that of **pCA $_7$** at δ_C/δ_H 144.8/7.51 ppm. To sum up, all the NMR signal assignments of these spectra (including acetylated and non-acetylated samples) are listed in Table 2.

LCC Linkages in the Bamboo Samples

Identification of various LCC linkages by using 2D NMR methods was an important milestone in LCC studies. A recent report suggested that CEL is the best preparation in order to evaluate benzyl ether LCC linkages [33]. The acetylated REB and RCEL were found to be similar in this

study; therefore, non-acetylated EB and REB were selected to detect the LCC linkages since the *in vivo* LCC probably adequately remained after enzyme hydrolysis. A previous study showed that benzyl ether (**BE**) LCC structures can be subdivided as follows [33]: (a) C1-linkages between the α -position of lignin and primary OH groups of carbohydrates (at C-6 of Glc, Gal, and Man and C-5 of Ara), giving a cross-peak at δ_C/δ_H 80–81/4.5–4.7 ppm and (b) C2-linkages between the α -position of lignin and secondary OH groups of carbohydrates, mainly of lignin-xylan type, giving a cross-peak at 80–81/5.1–4.9 ppm. As expected, two apparent signals, which are probably due to different kinds of benzyl ether LCC structures, were found at δ_C/δ_H 81.2/4.63 and 81.2/5.04 ppm in the spectra of EB and REB (shown in Fig. 10 and depicted in Fig. 11). The signal at δ_C/δ_H 81.2/5.04 ppm is probably overlapped with the α -position of spirodienone linkage in lignin according to previous studies [14, 33]. However, the other positions of spirodienone (such as β , 2, and 6 positions) were not found in the HSQC spectra (non-acetylated). This implied the absence of spirodienone linkage and further suggested the existence of benzyl ether LCC (lignin-xylan type) in the EB and REB.

The existing research showed that phenyl glycoside linkages (**PhGlc**) give a group of signals of carbohydrates C-1 at

δ_C/δ_H 104–99/4.8–5.2 ppm according to model compound data [34]. In the anomeric region (C_1-H_1) of the bamboo samples (EB, REB, and MWL), the signals for phenyl glycoside linkages were tentatively assigned according to previous literatures [33, 35]. These cross-signals were labeled as **PhGlc** in the spectra, and their correlations were observed at δ_C/δ_H 99.5/4.90, 100.0/5.10, and 101.9/4.89 ppm. Moreover, it was found that the phenyl glycoside linkages in MWL are more abundant than that of EB and REB. The reason for this could be attributed to the effect of cellulases, which was found to cleave the phenyl glycoside linkages [35]. Furthermore, the corresponding anomeric correlations of β -D-xylopyranoside units (**X₁**) were found at δ_C/δ_H 101.5/4.30 ppm, whereas the overlapped signals for anomeric correlations of (1→4)- β -D-glucopyranoside units (**Glc1**) might be observed at δ_C/δ_H 103.0/4.23 ppm in this region [5]. The anomeric correlations from the reducing end of (1→4)- α -D-xylopyranoside (**α X₁**) and (1→4)- β -D-xylopyranoside (**β X₁**) units were found at δ_C/δ_H 92.0/4.87 and 97.3/4.22 ppm, respectively [3].

The possible existence of ester LCC structures as well as γ -acetylated lignin should be discussed. That is, a possibility of overlapping LCC γ -esters signals with signals of various types of lignin γ -esters should be considered. In this study,

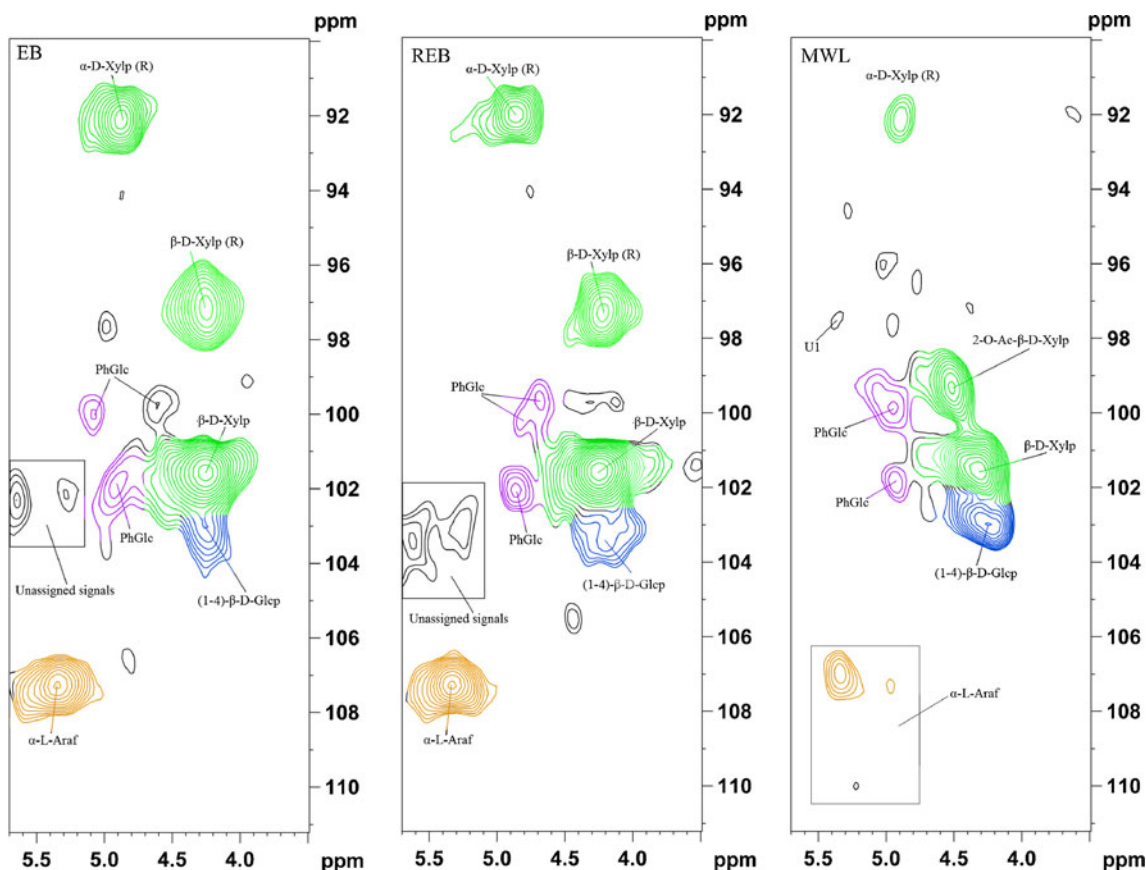
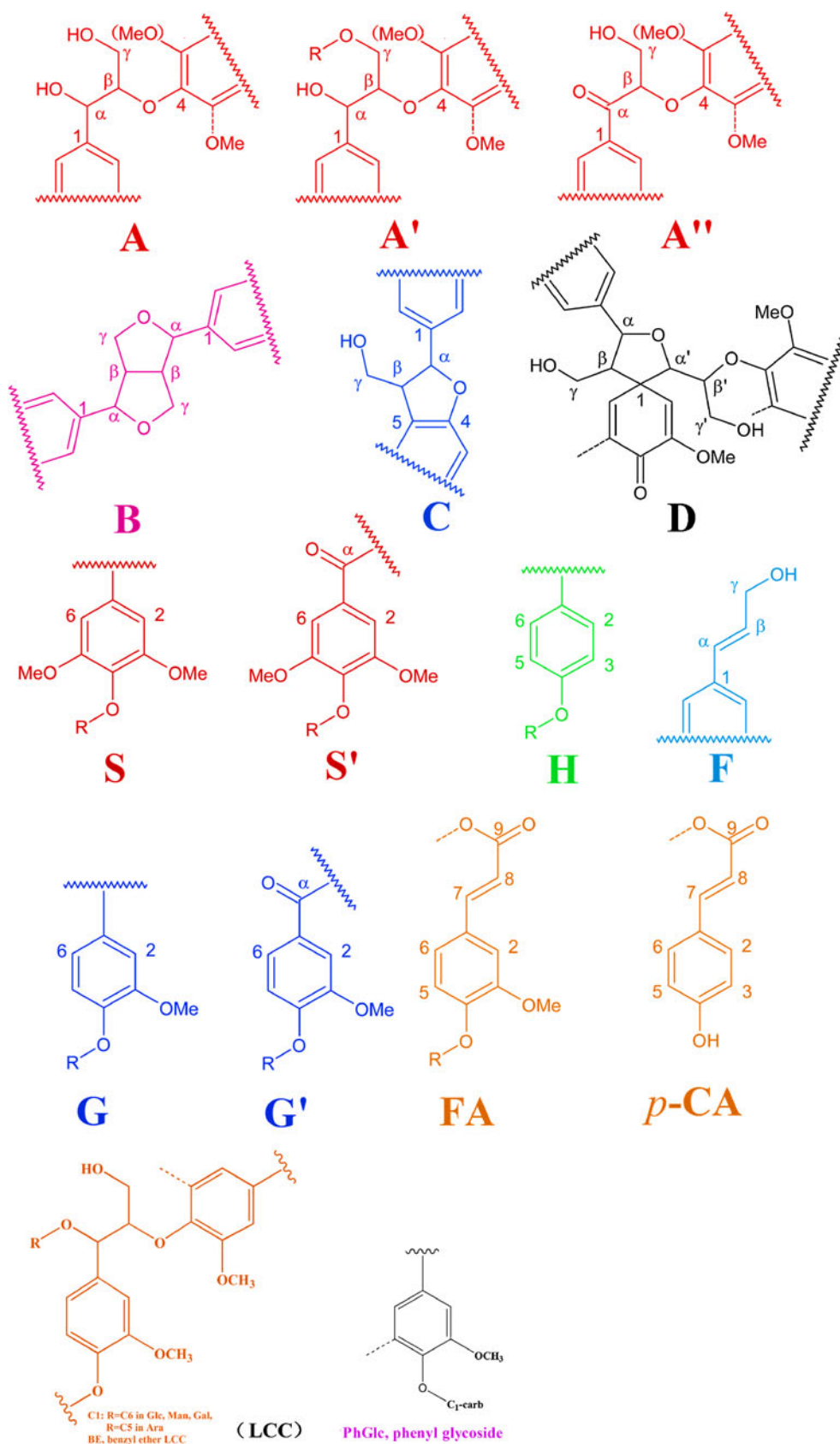


Fig. 10 The amplifying anomeric regions of HSQC spectra of EB, REB, and MWL (non-acetylated)

Fig. 11 Main lignin substructures in the treated bamboo samples (*A*) β -O-4 linkages; (*A'*) acylated β -O-4 substructures; (*A''*) C_α -oxidized β -O-4 linkages substructures (*B*) resinol structures formed by β - β / α - γ / γ -O- α linkages; (*C*) phenylcoumarane structures formed by β -5/ α -O-4 linkages; (*D*) spirodienone structures formed by β -1 linkages; (*S*) syringyl unit; (*S'*) oxidized syringyl unit linked a carbonyl or carboxyl group at C_α (phenolic); (*H*) *p*-hydroxyphenyl units; (*F*) *p*-hydroxycinnamyl alcohol end groups; (*G*) guaiacyl unit; (*G'*) oxidized guaiacyl units with a C_α ketone; (*FA*) ferulate; (*p-CA*) *p*-coumarate; (*LCC* linkages) possible lignin-carbohydrate linkages; (*PhGlc*) phenyl glycoside; (*BE*) benzyl ether



p-coumaric acid was found to acylate at the γ -position of the lignin side chain. Besides, acetate was found in the EB and REB at δ_C/δ_H 20.4/1.90 ppm, which generally acylated at C-2 and C-3 of xylans; however, the distinct signals for acetylated xylans were not found in the spectra. Therefore, the acetate observed was supposed to acylate at γ -position of the side chain of lignin. However, the existence of ester LCC structures (γ -position of the lignin–ester–glucuronic acid) in these samples (EB and REB) should be deeply studied in the future. In this study, the signals for glucuronic acid were not found. A possible reason for this could be ascribed to the non-detectable amount of the LCC linkage. Another explanation for this could be the esterase activity of cellulase because the ester-linked carbohydrates suffered the degradation under the enzymatic hydrolysis in the present study [28].

Quantitative Analysis of Lignin Structures in the Non-acetylated Bamboo Samples during Various Treatments

In order to maximize the utilization of enzymatic hydrolysis residue, the quantitative information of its structural features should be investigated. A recent published 2D HSQC NMR quantitative method was applied to estimate the lignin-coupling bond in hardwood and softwood samples [36]. The method uses as an internal standard a cluster of signals that are representative of all C₉ units present in the sample. In this study, the quantitative method was applied with minor modification. For grass lignin (bamboo lignin), the internal standard can thus be quantified by the total integration of the half syringyl signal (S_{2,6}) plus the G₂ signal as well as half of the integration of H_{2,6} cross signal.

$$I_{C9} \text{ units} = 0.5I_{S_{2,6}} + I_{G_2} + 0.5I_{H_{2,6}}(I_{C9})$$

where $I_{S_{2,6}}$ is the integration of S_{2,6}, and include S and S'; I_{G_2} is the integral value of G₂. $I_{H_{2,6}}$ is the integral value of H_{2,6}. I_{C9} represents the integral value of the aromatic ring. According to the internal standard (I_{C9}), the amount of $I_X\%$ could be obtained by the following formula:

$$I_X\% = I_X/I_{C9} \times 100\% \quad (1)$$

where I_X is the integral value of α -position of **A** (β -O-4), **B** (β - β), and **C** (β -5); the integration should be conducted in the same contour level. However, it should be noted that the accuracy of 2D HSQC quantitative results depends on the resolution of the signals representing for different substructures.

Based on Eq. 1, the relative volumes of the contour peaks, which are also the implied relative concentrations of the each linkage bonds, such as β -aryl ether (**A**, β -O-4), resinol (**B**, β - β), and phenylcoumaran (**C**, β -5), and their abundances were estimated quantitatively and listed in Table 3. It was found that the frequencies of β -O-4 coupling bonds in all the samples ranged from 47.53–54.55/

Table 3 Quantitative characteristics of the lignin polymer in the treated bamboo samples by in situ NMR technique

Sample	β -O-4 ^a	β - β ^a	β -5 ^a	S/G ^b
Ac-B	51.11	0.95	ND	1.42
Ac-RB	48.95	0.81	0.45	1.36
Ac-EB	54.55	5.48	3.45	1.35
Ac-REB	50.97	2.78	1.67	1.61
Ac-RCEL	52.50	2.02	0.88	1.71
Ac-RREL	47.96	1.12	ND	1.80
EB	47.68	6.60	2.65	1.37
REB	47.53	5.33	3.58	1.60
MWL	49.01	7.07	2.17	1.77

ND not detected

^a Results express per 100 Ar based on quantitative 2D NMR (Eq. 1)

^b S/G ratio obtained by this equation: S/G ratio = $I_{S_{2,6}}/2/I_{G_2}$

100Ar. The amounts of β -O-4 linkage were observed to be high in Ac-RB and Ac-REB as compared to that of Ac-B and Ac-EB. This suggests that Ac-B and Ac-EB are more degraded preparations, whereas Ac-RB and Ac-REB undergone less degradation from the bamboo samples studied. As expected, the content of β -O-4 in Ac-REB was between that of Ac-RCEL and Ac-RREL because REB was fractionated into RCEL and RREL. Moreover, the content of β -O-4 linkage in REB, RCEL, and RREL was decreased in the order of Ac-RCEL > Ac-REB > Ac-RREL (Table 3).

The different S/G (syringyl to guaiacyl) ratios in the samples studied (Table 3) are caused by fractionation during different handling processes [33]. It is worth estimating the S/G ratio of the different bamboo samples during the regenerated and enzymatic process. It was estimated that the S/G ratios for B and RB were 1.63 and 1.46, respectively. The lower S/G ratio of RB was probably due to the removal of a small lignin fragment rich in S units during the regenerated process. Similar result indicated that S-rich lignin fragments were firstly released during the delignification process [14]. However, after enzymatic treatment, the S/G ratios for acetylated EB and REB were estimated to be 1.37 and 1.61, respectively. Similar S/G ratios were observed in the non-acetylated bamboo samples (EB and REB, Table 3). In addition, the S/G ratios of RCEL and RREL (from REB) were calculated to be 1.71 and 1.80, respectively. Interestingly, it was found that the residue RREL was abundant with S units in this study. This was in agreement with a recent report [37]. They also found that ASAM residual lignin from beech wood was rich in syringyl units. On the basis of higher S/G ratio and non-detectable amount of condensed unit β -5 (REL), a likely speculation is that RREL contained less condensed units than those of RCEL and REB. Furthermore, the different chemical reactivities between syringyl and guaiacyl units ($R_S < R_G$) also added some clues to such low amount of condensed units.

Coincidentally, a previous report also indicated that REL has less condensed units than that of MWL [8].

Conclusion

The chemical composition changes of bamboo during successive treatments were characterized by in situ HSQC NMR technique without component isolation. The regenerated cell wall showed higher enzymatic efficiency than the original bamboo. However, the obstinate cellulose still remained in the RREL, suggesting that the cellulose was not easily degraded even after regeneration process. In addition, the fact that the acetyl groups linked to xylans were cleaved during treatment with cellulase suggested that the esterifiable acetyl groups were sensitive to cellulase (celluclast 1.5 L), and the cellulase preparation probably possesses esterase activity.

Another important objective is that unveiling the structural heterogeneity of lignin during enzymatic treatment by in situ NMR (HSQC) techniques (acetylated and non-acetylated samples) was also successfully performed. The major lignin substructures (β -O-4, β - β , and β -5) and various LCC linkages (benzyl ether and phenyl glycosidic linkages) were assigned in the successively treated samples. In addition, the various frequencies of β -O-4, β - β , and β -5 linkages and S/G ratios in all the samples were quantitatively obtained via in situ HSQC NMR spectra. Furthermore, the RREL contained a larger amount of syringyl units and less condensed units as compared to those of RCEL and REB. Therefore, in situ characterization by HSQC NMR analysis is a beneficial structural analysis methodology in the emerging biomass research field for the characterization of pretreated biomass and enzymatic hydrolysis lignin.

Acknowledgements The authors are extremely grateful to financial support from Major State Basic Research Projects of China (973-2010CB732204, 2012CB215302) and Natural Science Foundation of China (31110103902).

References

- Ragauskas AJ, Williams CK, Davison BH et al (2006) The path forward for biofuels and biomaterials. *Science* 311:484–489
- Lu FC, Ralph J (2011) Solution-state NMR of lignocellulosic biomass. *J Biobased Mater Bio* 5:169–180
- Kim H, Ralph J (2010) Solution-state 2D NMR of ball-milled plant cell wall gels in DMSO- d_6 /pyridine- d_5 . *Org Biomol Chem* 8:576–591
- Martínez AT, Rencoret J, Nieto L, Jiménez-Barbero J, Gutiérrez A, del Río JC et al (2011) Selective lignin and polysaccharide removal in natural fungal decay of wood as evidenced by in situ structural analyses. *Environ Microbiol* 13:96–107
- Samuel R, Foston M, Jaing N, Allison L, Ragauskas AJ (2011) Structural changes in switchgrass lignin and hemicelluloses during pretreatments by NMR analysis. *Polym Degrad Stab* 96:2002–2009
- Samuel R, Foston M, Jaing N, Allison L, Cao SL, Allison L et al (2011) HSQC (heteronuclear single quantum coherence) ^{13}C - ^1H correlation spectra of whole biomass in perdeuterated pyridinium chloride–DMSO system: an effective tool for evaluating pretreatment. *Fuel* 90:2836–2842
- Lu FC, Ralph J (2003) Non-degradative dissolution and acetylation of ball-milled plant cell walls: high-resolution solution-state NMR. *Plant J* 35:535–544
- Holtman KM, Chang HM, Kadla JF (2007) An NMR comparison of the whole lignin from milled wood, MWL, and REL dissolved by the DMSO/NMI Procedure. *J Wood Chem Technol* 27:179–200
- Colombini MP, Lucejko JJ, Modugno F, Orlandi M, Tolppa EL, Zoi L et al (2009) A multi-analytical study of degradation of lignin in archaeological waterlogged wood. *Talanta* 80:61–70
- Salanti A, Zoia L, Tolppa EL, Giachi G, Orlandi M (2010) Characterization of waterlogged wood by NMR and GPC techniques. *Microchem J* 95:345–352
- Qu C, Kishimoto T, Kishino M, Hamada M, Nakajima N (2011) Heteronuclear single-quantum coherence nuclear magnetic resonance (HSQC NMR) characterization of acetylated Fir (*Abies sachalinensis* MAST) wood regenerated from ionic liquid. *J Agr Food Chem* 59:5382–5389
- Kim H, Ralph J, Akiyama T (2008) Solution-state 2D NMR of ball-milled plant cell wall gels. *Bioenerg Res* 1:56–66
- Yelle DJ, Ralph J, Frihart CR (2008) Characterization of nonderivatized plant cell walls using high-resolution solution-state NMR spectroscopy. *Magn Reson Chem* 46:508–517
- Wen JL, Sun ZJ, Sun YC, Sun SN, Xu F, Sun RC et al (2010) Structural characterization of alkali-extractable lignin fractions from bamboo. *J Biobased Mater Bio* 4:408–425
- Björkman A (1956) Studies on finely divided wood. Part 1. Extraction of lignin with neutral solvents. *Svensk Papperst 59:477–485*
- Zhang AP, Lu FC, Sun RC, Ralph J (2010) Isolation of cellulolytic enzyme lignin from wood preswollen/dissolved in dimethyl sulfoxide/*N*-methylimidazole. *J Agr Food Chem* 58:3446–3450
- Pan XJ, Kadla JF, Ehara K, Neil G, Saddler JN (2006) Organosolv ethanol lignin from hybrid poplar as a radical scavenger: relationship between lignin structure, extraction conditions, and antioxidant activity. *J Agr Food Chem* 54:5806–5813
- Heikkinen S, Toikka MM, Karhunen PT, Kilpeläinen IA (2003) Quantitative 2D HSQC (Q-HSQC) via suppression of *J*-dependence of polarization transfer in NMR spectroscopy: application to wood lignin. *J Am Chem Soc* 125:4362–4367
- Mario F, Schröder P, Wollboldt RP, Weber HK, Sixta H (2008) A new and facile method for isolation of lignin from wood based on complete wood dissolution. *Holzforschung* 62:15–23
- Chen Y, Shimizu Y, Takai M, Hayashi J (1995) A method for isolation of milled-wood lignin involving solvent swelling prior to enzyme treatment. *Wood Sci Technol* 29:295–306
- Jääskeläinen AS, Sun Y, Argyropoulos DS, Tamminen T, Hortling B (2003) The effect of isolation method on the chemical structure of residual lignin. *Wood Sci Technol* 37:91–102
- Xie HB, King A, Kilpeläinen I, Granström M, Argyropoulos DS (2007) Thorough chemical modification of wood-based lignocellulosic materials in ionic liquids. *Biomacromolecules* 8:3740–3748
- Schwanninger M, Rodrigues JC, Pereirac H, Hinterstoisser B (2004) Effects of short-time vibratory ball milling on the shape of FT-IR spectra of wood and cellulose. *Vib Spectrosc* 36:23–40
- Faix O (1991) Classification of lignins from different botanical origins by FT-IR spectroscopy. *Holzforschung* 45:21–27
- Hedenström M, Wiklund-Lindström S, Öman T et al (2009) Identification of lignin and polysaccharide modifications in *Populus*

- wood by chemometric analysis of 2D NMR spectra from dissolved cell walls. *Mol Plant* 2:933–942
26. Higuchi T (1987) Chemistry and biochemistry of bamboo. *Bamboo J* 4:132–145
 27. Wen JL, Sun YC, Xu F, Sun RC (2010) Fractional isolation and chemical structure of hemicellulosic polymers obtained from *Bambusa rigida* species. *J Agr Food Chem* 58:11372–11383
 28. Juhást T, Szengyel Z, Réczey K, Siika-Aho M, Viikari L (2005) Characterization of cellulases and hemicellulases produced by *Trichoderma reesei* on various carbon sources. *Process Biochem* 40:3519–3525
 29. Lu FC, Ralph J (1999) Detection and determination of *p*-coumaroylated units in lignins. *J Agr Food Chem* 47:1988–1992
 30. Ralph J, Lu FC (1998) The DFRC method for lignin analysis. 6. A simple modification for identifying natural acetates on lignins. *J Agr Food Chem* 46:4616–4619
 31. Zhang AP, Lu FC, Liu CF, Sun RC (2010) Isolation and characterization of lignins from *Eucalyptus tereticornis* (12ABL). *J Agr Food Chem* 58:11287–11293
 32. Yuan TQ, Sun SN, Xu F, Sun RC (2011) Characterization of lignin structures and lignin-carbohydrate complex (LCC) linkages by quantitative ^{13}C and 2D HSQC NMR. *J Agr Food Chem* 59:10604–10614
 33. Balakshin M, Capanema E, Gracz H, Chang HM, Jameel H (2011) Quantification of lignin-carbohydrate linkages with high-resolution NMR spectroscopy. *Planta* 233:1097–1110
 34. Enoki A, Yaku F, Koshijima T (1983) Synthesis of LCC model compounds and their chemical and enzymatic stabilities. *Holzfoschung* 37:135–141
 35. Ibarra D, Chávez MI, Rencoret J et al (2007) Structural modification of eucalypt pulp lignin in a totally chlorine free bleaching sequence including a laccase-mediator stage. *Holzforschung* 61:634–646
 36. Sette M, Wechselberger R, Crestini C (2011) Elucidation of lignin structure by quantitative 2D NMR. *Chem Eur J* 17:9529–9535
 37. Choi JW, Faix O (2011) NMR study on residual lignins isolated from chemical pulps of beech wood by enzymatic hydrolysis. *J Ind Eng Chem* 17:25–28